

# On the Imaging Speed of Wideband Direct Detection FPAs

S.L. van Berkel, O. Yurduseven, A. Freni, A. Neto and N. Llombart  
Tera-Hertz Sensing Group, Dept. of Microelectronics, TU Delft, The Netherlands

**Abstract**—This paper presents an analysis of the imaging speed in millimeter and sub-millimeter wave imaging systems when a broad portion of the THz spectrum is utilized. The imager is based on a large focal plane array (FPA) of incoherent detectors. The detectors are assumed to be uncooled such that the system is operating in a detector-noise limited scenario. The Signal-to-Noise (SNR) ratio increases then linearly with bandwidth. The imaging speed is assessed in terms of *effective bandwidth* and the resolution with the *effective reflector patterns*. The imaging speed and resolution of a FPA, based on recently developed wideband (1:5 relative bandwidth) leaky-lens antennas, is compared relatively to the speed and resolution of a horn antenna FPA (1:1.5 relative bandwidth). The analysis will show that, ultimately, maximizing the imaging speed will be in trade-off with the resolution.

## I. INTRODUCTION

Millimeter or sub-mm-wave imaging detector arrays are readily available [1] and can be implemented coherently [2] or incoherently [3] (i.e. direct detection). In this contribution we focus on incoherent detection architectures which require a quasi-optical system in combination with a FPA in order to generate the image. Typically a high imaging speed is achieved by cryogenically cooling the detectors. However, practical speeds can also be achieved by using many receivers utilizing a broad portion of the THz-band. This leads to uncooled integrated detection solutions suitable for low-cost imaging applications. For direct detection schemes the SNR, after  $\tau_{int}$  seconds of integration by the detector, can be expressed as [4]:

$$SNR = \frac{P_a}{NEP} \sqrt{\tau_{int}} \quad (1)$$

where, the  $NEP$  is the Noise Equivalent Power. The expression of the SNR (1) follows from the  $NEP$ , which is defined as the amount of input power that is necessary to equate the RMS noise power fluctuations after 1s of integration, making the SNR=1. Without performing any mechanical scanning, the imaging speed,  $s$ , is defined as  $s = \frac{1}{\tau_{int}}$  and is then quadratically depending on the received power  $P_a$ :  $s = (\frac{P_a}{NEP})^2$ . The key observable parameter in radiometric systems is the spectral brightness distribution  $B(f, \Omega)$  of incoherent sources at a temperature  $T$  and can be described by Planck's law. We assume that the radiometer is operating in the Rayleigh-Jeans limit with respect to the source,  $hf \ll k_B T$ , allowing for an approximation on the spectral brightness:

$$B(f, \Omega)|_{hf \ll k_B T} = \frac{f^2}{c^2} k_B T(\Omega) \quad (2)$$

with  $f$  the frequency,  $c$  the speed of light,  $h$  Planck's constant and  $k_B$  being Boltzmann's constant. The received

power by the  $n$ -th antenna feed  $P_a^n$  can be expressed as an integration of the spectral brightness (2) over the operational bandwidth  $BW_{RF} = f_{max} - f_{min}$  and over the source solid angle  $\Omega_s$ , viewed and weighted by the effective area  $A_{eff}^R(f, \Omega)$  of the reflector system:

$$P_a^n = \int_{f_{min}}^{f_{max}} \int_{\Omega_s} A_{eff}^R(f, \Omega - \Omega_n) B(f, \Omega) d\Omega df \quad (3)$$

Focusing on the on-axis element ( $n = 0$ ), the effective area of the antenna radiometer can be related to the directivity  $D^R(f, \Omega)$ ;  $A_{eff}^R(f, \Omega) = \frac{c^2}{f^2} \frac{1}{4\pi} \eta_{opt}(f) D^R(f, \Omega)$ , where  $\eta_{opt}(f) = \eta_{feed}(f) \eta_{so}^{\Omega_R}(f)$  is the system's optical efficiency. The optical efficiency consists out of general feed-efficiencies  $\eta_{feed}(f)$  while a more significant contribution is the spill-over efficiency w.r.t. the reflector solid angle  $\eta_{so}^{\Omega_R}(f)$ . The spill-over efficiency defines how well the antenna feed pattern is coupled with the angle spanned by the reflector  $\Omega_R$ . Substituting the effective area and (2) in (3) leads to

$$P_a = \frac{k_B}{4\pi} \int_{\Omega_s} T(\Omega) G_{eff}(\Omega) d\Omega \quad (4a)$$

$$G_{eff}(\Omega) = \int_{f_{min}}^{f_{max}} \eta_{opt}(f) D(f, \Omega) df \quad (4b)$$

$G_{eff}$ , being the effective reflector gain, is obtained by weighting the spectral directivity by the optical efficiency of the reflector system and integrating over the operational bandwidth. In order to have a convenient way to compare the imaging speed for different FPA architectures we assume to have an average temperature of  $T_S^{ave}$  over the full solid angle and that the sources are distributed so that the integration of the spectral directivity over source solid angle is  $4\pi$ . The average received power by the feed can now be written as (5a) where we have defined the effective bandwidth as (5b).

$$P_a^{ave} \approx k_B T_S^{ave} BW_{RF}^{eff} \quad (5a)$$

$$BW_{RF}^{eff} = \int_{f_{min}}^{f_{max}} \eta_{opt}(f) df \quad (5b)$$

The average received power is linearly depending on this effective bandwidth, resulting in quadratic dependence for the imaging speed  $s \propto (BW_{RF}^{eff})^2$ . We will compare the effective bandwidth  $BW_{RF}^{eff}$  and effective reflector gain  $G_{eff}(\Omega)$  of recently developed leaky lens antenna's [5] in a 1:5 frequency

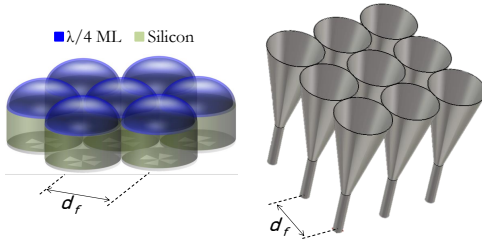


Fig. 1. Leaky-lens antennas as developed in [5] and circular horn antenna's sampled identically. The feeds are used in an FPA of a reflector system with  $F_{\#} = 2.5$

band with respect to conventional 1:1.5 relative bandwidth horn-antennas. The feeds are shown in Figure 1.

## II. RESULTS

In order to have a fully sampled image of the source region, the feeds in the FPA should be sampled at  $d_f = 0.5F_{\#}\lambda_s$  [6]. Here  $\lambda_s$  is the wavelength at the sampling frequency  $f_s$ ,  $F_{\#} = F/D$  is the ratio of the focal distance  $F$  with diameter  $D$  of the optics. As we will see, maximizing the imaging speed implies that the feeds should be sampled at the lowest frequency resulting in an under-sampled array for higher frequencies.

Let us evaluate a reflector system with  $F_{\#} = 2.5$  containing a 1:5 relative bandwidth FPA based on leaky-lens antenna feeds as is developed in [5] and shown in Figure 1. The feeds are optimized and analyzed by numerical CST-simulations and are placed in a fully sampled array ( $d_f = 0.5F_{\#}\lambda_s$ ) w.r.t. the lowest operating frequency  $f_s = f_{min}$ . The feed-efficiency, spill-over efficiency w.r.t. the reflector and optical efficiency are shown in Figure 2 by the solid lines. The average optical efficiency is 45%, leading to an effective bandwidth (5b) of  $BW_{RF}^{eff} = 1.81f_s$ . It is clear that the wideband feeds mainly integrate power from the upper portion of the spectrum where the array is under-sampled. The trade-off in resolution becomes clear when observing the normalized effective reflector gain (4b) in Figure 3. Both E- and H-planes are shown by the solid lines for three adjacent feeds ( $n = 0, \pm 1$ ). The patterns overlap at approximately -8dB. This implies that the focal plane is actually not fully sampled and the bandwidth is solely used to maximize power. In fact, one could also say that the array is *maximum gain sampled* at  $f'_s = 4f_s$ ;  $d_f = 2F_{\#}\lambda'_s$  but without any mechanically scanning. To illustrate this statement, let us compare the results with a 1:1.5 FPA containing circular horn-antenna's, sampled identically to the leaky-lens antennas with  $d_f = 2F_{\#}\lambda'_s$ . The horn-antenna's are operating in a 1:1.5 relative bandwidth from  $\frac{10}{3}f_s \rightarrow 5f_s$  as indicated in Figure 2. The efficiencies are shown by the dashed lines. The horn antennas are simulated without any losses or feeding network. Instead we define the feed efficiency optimistically at 90% over the full band. The average optical efficiency is 61.9% leading to an effective bandwidth of  $BW_{RF}^{eff} = 1.03f_s$ . For distributed sources the leaky-lens based FPA will be faster with a factor of

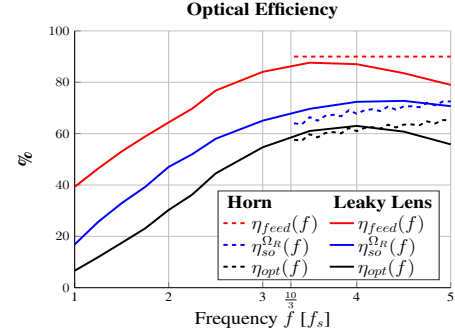


Fig. 2. Optical efficiency for both the leaky-lens FPA and horn FPA.

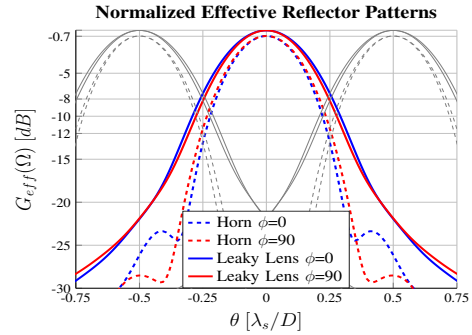


Fig. 3. Effective reflector patterns normalized to  $G_{eff}^{Leaky Lens}(\theta = 0)$  for three adjacent feeds ( $n = 0, \pm 1$ ).

$\frac{s_{Leaky-Lens}}{s_{Horn}} = \left(\frac{1.81f_s}{1.03f_s}\right)^2 = 3.09$ . The effective reflector patterns are indicated in Figure 3 by the dashed lines. Patterns of adjacent feeds overlap at -12dB; the focal-plane is indeed under-sampled in order to gain in imaging speed.

This analysis showed that maximizing the imaging speed for a wideband FPA implies that resolution will be traded-off.

## ACKNOWLEDGEMENT

This research is supported by the Dutch Technology Foundation STW. N. Llombart thanks the European Research Council (ERC) for the starting grant LAA-THz-CC (639749). The work of A. Neto was supported by ERC Consolidator Grant AAATSI (278794).

## REFERENCES

- [1] R. A. Hadi, et. al., "A 1 k-pixel video camera for 0.7-1.1 Terahertz imaging applications in 65-nm cmos," *IEEE Journal of SSC*, vol. 47, no. 12, pp. 2999-3012, 2012.
- [2] J. W. May, "SiGe integrated circuits for millimeter-wave imaging and phased arrays," Thesis, 2009. [Online]. Available: <http://www.escholarship.org/uc/item/5488f0g9>
- [3] P. L. Richards, "Bolometers for infrared and millimeter waves," *Journal of AP*, vol. 76, no. 1, pp. 1-24, 1994.
- [4] P. H. Siegel and R. J. Dengler, "Terahertz heterodyne imaging part i: Introduction and techniques," *International Journal of Infrared and Millimeter Waves*, vol. 27, no. 4, pp. 465-480, 2006.
- [5] O. Yurduseven, N. Llombart, and A. Neto, "A dual-polarized leaky lens antenna for wideband focal plane arrays," *IEEE TAP*, vol. 64, no. 8, pp. 3330-3337, 2016.
- [6] J. F. Johansson, "Millimeter-wave imaging theory and experiments," *Onsala Space Observatory Research Report, No. 151, 1986*, vol. 1, p. 1, 1986.